Estimating 3-Space Velocity from REG-REG Correlations

Peter C. Morris
Adelaide, South Australia. April 26, 2016
E-mail: ptr.mrrs@tpg.com.au

"Nanotechnology Quantum Detectors for Gravitational Waves. . . ", *Progress in Physics*, 2013, v. 4, 57-62 [1], describes detection of gravitational dynamical 3-space waves through correlation analysis of data from quantum Random Event Generators (REGs) operating within the Global Consciousness Project (GCP) network. We found this extremely interesting so attempted to perform similar analysis using different data from the same network. We were able to extract correlations such as those reported, estimate the velocities of 3-space waves and 3-space flow and observe earth orbit aberration effects. Herein we describe our analysis and results.

1 Introduction

In dynamical 3-space theory [1], gravity is caused by acceleration of space into matter. The equations governing this process are nonlinear and lead to the prediction of dynamical 3-space waves. These are a type of gravitational wave but they differ from those predicted by General Relativity.

Random Event Generator (REG) devices generate supposedly random numbers by detecting the quantum to classical transition of electrons tunnelling through a barrier in a tunnel diode. According to the standard interpretation of quantum theory the electron current fluctuations caused by such transitions should be completely random, however observations in [1] imply that this is not the case and that the quantum to classical transitions are being induced by dynamical 3-space fluctuations. The passage of 3-space waves though such devices may then induce electron current fluctuations that allow their passage to be detected.

Dynamical 3-space theory predicts that 3-space waves refract as 3-space accelerates into gravitating bodies. This implies that inflows into the Sun, Earth and Moon will cause waves that were planar in form to become less-planar as they near Earth prior to detection by REG devices. To minimize the presence of such effects in our data, we analysed REG data from days when the Sun and Moon were on approximately opposite sides of the Earth, as their inflow effects could then partially cancel rather than add and allow refraction effects to be more symmetrical with respect to determinations of incoming wave directions and speeds.

We then obtained data from a GCP REG located in Perth, Australia and from another in Manchester, U.K.*, as shown in Table 1 for all full moon and adjacent days for which data was available from 1 July 2012 to 30 June 2013.

Of 39 potential days, complete data was available for 29.

Table 1: Details of GCP REG Devices Used

	Perth	Manchester
ID Number	2232	2006
Latitude	-31.921	53.682
Longitude	115.892	-2.165
Device Type	Orion	Orion

2 Travel times

For each of the above mentioned 29 days, Perth to Manchester travel time τ values were determined by computing the correlation function†,

$$C(\tau, t) = \sum_{t'=t-T}^{t'=t+T} S_1[t' - \lfloor \tau/2 \rfloor] \, S_2[t' + \lceil \tau/2 \rceil] \, e^{-a(t'-t)^2} \qquad (1)$$

for data sequences $S_1[t]$ and $S_2[t]$ containing values output once per second by the REG devices. Here $\lfloor \rfloor$ and $\lceil \rceil$ represent floor and ceiling functions that round $\tau/2$ down or up to integer values to ensure correct indexing when τ is an odd number. $2T = 200s$ is the time interval used about UTC time t, and the Gaussian term applies a Gaussian window.

Parameter a needs to be chosen to make the window narrow enough to suppress end effects but broad enough to allow enough terms to contribute to the sum. We obtained consistent results using $0.00037 \le a \le 0.00042$, but a sharp improvement of signal to noise ratio (S/N) at $a = 0.00038$ suggested that this could be the optimum value and was used to derive the final results reported herein.

τ values were determined by calculating $C(\tau, t)$ for τ in the range 9 to 23 seconds and then finding which value of τ in the range 10 to 22 corresponded to the maximum peak value of $C(\tau, t)$.

Travel times with high correlations‡ were then binned and averaged per RA hour of the Manchester-Perth spatial separa-

*We think these are the same pair of REGs mentioned in [1]. There can be no ambiguity about the Perth REG as there is only one. However the GCP web site [4] has two entries for REG 2006. The first puts it at London from 2001 onward and the second as near Manchester from 2006 onward. The second entry is easy to miss, so the London REG referred to in [1] may have been REG 2006 located near Manchester.

†Derived from equation (2) in [1].

‡For each day the high correlations were all those higher than a cut-off value which would allow each bin to contain at least one sample. To the bin(s) which then contained only one sample, a second sample with the

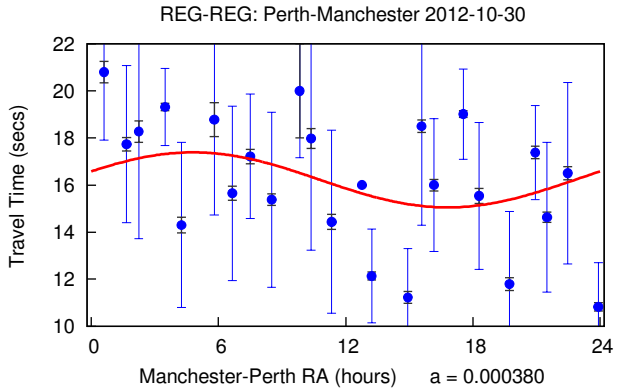

Fig. 1: Travel times from REG-REG Perth to Manchester data for October 30, 2012. High correlation values for each Manchester-Perth RA hour have been binned and the mean, SD (blue) and SEM (grey) shown. The red curve shows a least square error best fit of a sinusoid to all points. RA of each point is the mean RA of values in the associated bin causing horizontal spacing of points to be non-uniform.

tion vector, that rotates with the Earth. We thereby obtained a mean travel time, Standard Deviation (SD) and Standard Error in the Mean (SEM) for 24 RA directions, such as shown in Fig. 1, for each of the 29 days.

The SDs varied from zero to large. Large SDs could be caused by excessive detection of waves from multiple directions during an hour which could degrade results, so to reduce such effects in our analysis we calculated a median travel time SD for each day and selected for further consideration the 60% of days with the smallest median SDs. This left us with data for 17 days for further analysis.

3 Fitting of sinusoids

Given travel time data for 24 RA directions, the incoming speed and the direction of plane waves can be determined by fitting,

$$\tau = \frac{\mathbf{R} \cdot \mathbf{v}}{\mathbf{v}^2} \qquad (2)$$

where **R** is the Manchester-Perth spatial separation vector and **v** is the velocity of the Earth relative to the waves. As the daily rotation of **R** causes the right hand side of Eqn. (2) to be sinusoidal, the fit can be done by fitting a sinusoid to the travel times such as shown in Fig. 1.

The RA of the peak will then indicate the incoming RA of the waves and the amplitude and mean will allow determination of incoming declination and speed. However, the amplitude needs to be multiplied by a suitable factor to compensate for attenuation by noise.

nearest slightly lower correlation was added to allow calculation of standard deviation, but this had only a minor effect on results.

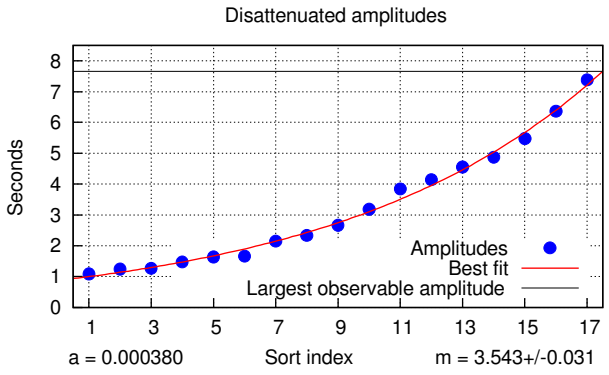

Fig. 2: Example of disattenuated amplitudes obtained by sorting the original values and then multiplying by a suitable value m to allow the best fit exponential curve to end at the largest observable amplitude.

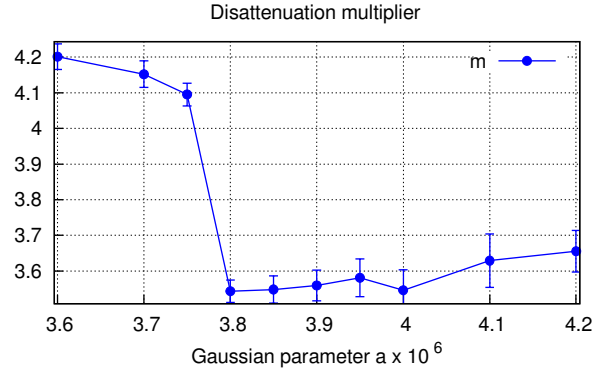

Fig. 3: Values of disattenuation multiplier m required when using different values of Gaussian parameter a. A smaller multiplier corresponds to better signal to noise ratio.

4 Amplitude disattenuation

Detection of waves from multiple directions is expected to cause randomness in travel time data even when one direction dominates. Then the averaging and sinusoid fitting procedures will cause random and signal values to be averaged together. In principle this will cause extracted signal amplitudes to be attenuated by an amount equal to $1/(1+n)$ where n is the average number of random values per signal value.

To compensate for this effect we multiplied the amplitudes of the fits so that a best fit of an exponential curve to a sorted list of the final values terminated at the amplitude of the largest sinusoid that could be fit to a waveform clipped to the τ range of 10 to 22. This "largest observable amplitude" turned out to be 7.66.

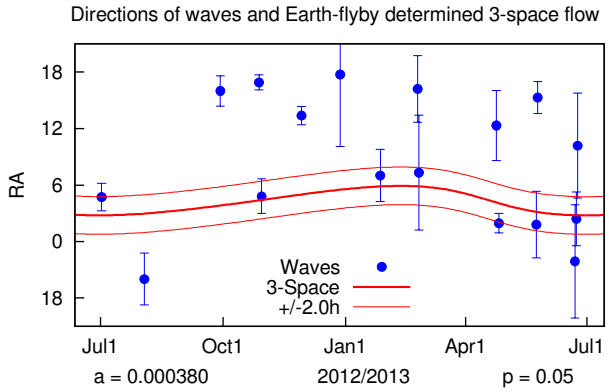

Fig. 4: Each point shows the average incoming RA of detected 3-space waves on a particular day. The red curve shows the RA of the Flyby orbital aberration circle depicted in Fig 11 in [2]. Six of the 17 points lie within ±2.0 RA hours of this curve. The probability of this being due to chance is $P = 0.05$, but is consistent with 3-space Earth orbit effects reported in [2] if waves more parallel to 3-space flow are preferentially detected.

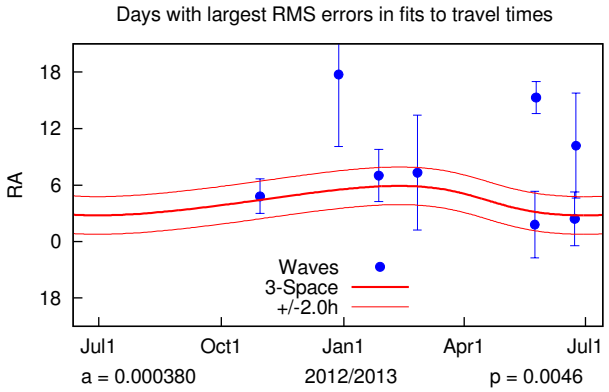

Fig. 5: Same as Fig. 4, but only showing the eight days when larger RMS errors in the fits of sinusoids to travel times suggested that wave velocities might have been more affected by gravitational inflow, due to being more parallel to 3-space flow. Five of the eight points lie within ±2.0 RA hours of the orbital aberration curve. The probability of this being due to chance is only $P = 0.0046$, but is consistent with gravitational inflow effects reported in [1] and Earth orbit effects [2].

Fig. 2 shows the disattenuated amplitudes obtained in this way for $a = .00038$ while Fig. 3 shows the multipliers that were required for different values of Gaussian parameter a. A sudden decrease corresponding to an increase of S/N occurs at $a = 0.00038$ so we choose this value of a to calculate our final results.

It can be noted that the value of $m = 3.54$ for $a = 0.00038$ corresponds to $n = (m - 1) = 2.54$ random values per signal value.

5 Wave RAs versus 3-space flow RA

For each of the 17 days selected as above, the average incoming wave RA was found from the peak of the sinusoid that best fit the travel times. These RA values are plotted in Fig. 4.

Also shown in Fig. 4 is a curve which shows how the incoming RA of 3-space flow would theoretically vary as the Earth moved in its orbit [5] for the case of an incoming galactic flow of RA = 4.29 hrs, dec = -75^0, speed = 486 km/s, which was the velocity determined in [2] by combining optical fiber light-speed data with spacecraft Earth-flyby radar doppler-shift data.

To derive the curve, the velocity of Earth relative to incoming 3-space was calculated using,

$$\mathbf{v} \approx \mathbf{v}_G - \mathbf{v}_{inS} + \mathbf{v}_{orbit} - \mathbf{v}_{inE} \qquad (3)$$

where $\mathbf{v}_G$ is the velocity of the Sun relative to distant galactic space, $\mathbf{v}_{inS}$ is velocity due to acceleration of 3-space towards the Sun, $\mathbf{v}_{orbit}$ is the orbital velocity of the Earth and $\mathbf{v}_{inE}$ is velocity due to acceleration of 3-space towards the Earth. Approximate vector addition of these components is possible because at the Earth's orbital positions, $\mathbf{v}_G$, $\mathbf{v}_{inS}$ and $\mathbf{v}_{orbit}$ are approximately orthogonal and $\mathbf{v}_{inE}$ represents a relatively small Earth directed effect that can be modeled as causing a speed increase. (Rigorous justification for vector addition of these components can be found in [3].)

6 Preferential detection of waves parallel to 3-space flow

Inspection of Fig. 4 reveals that six of the 17 points lie within ±2.0 RA hours of the RA of the 3-space curve. However if we were to assume that wave RAs are evenly distributed, we would expect only $17 \times \frac{4}{24} \approx 3$ points to lie this close to the curve. This suggests that waves more parallel to 3-space flow are being preferentially detected. The probability of this distribution being due to chance is only $P = 0.05^*$, but is consistent with 3-space Earth orbit effects reported in [2].

*The probability was calculated using the formula,

$$P = \sum_{k=r}^{n} \binom{n}{k} p^k (1-p)^{n-k}$$

where r is the number of points within ±2.0 RA hours of the curve, n is the total number of points and $p = 1/6$ is the probability of a point lying within ±2.0 RA hours of the curve if the distribution was random.

7 A test for gravitational inflow effects

If the REG devices were detecting plane waves in a static ether, rotation of **R** would allow travel times to fit a sinusoid for all 24 of the RA hours. However in the case of the waves considered here, it was reported in [1] that acceleration of 3-space into the Earth causes travel times to depart from sinusoidal form during RA hours when waves reach the second detector via deeper paths through the Earth. This effect will be greater for waves with velocities more parallel to the direction of flow, because in the case of orthogonal velocities, the accelerating flow would cause the wavefronts to slide sideways rather than accelerate forwards. This suggests that RMS errors in the fits should tend to be larger on days when wave velocities are more parallel to the direction of 3-space flow. To test for this inflow effect, we selected for further consideration the eight days whose sinusoid fits resulted in the largest RMS errors. If the hypothesis is correct this should leave us with a higher proportion of points within ±2.0 RA hours of the 3-space curve. The results plotted in Fig. 5 show that this is the case, because while five points still lie within ±2.0 RA hours of the curve only three now lie outside this range. The probability of this new distribution being due to chance is only $P = 0.0046$, but is consistent with gravitational inflow and Earth orbit effects [1, 2].

8 Incoming declination and speed

If we let τ_{mean} and τ_{amp} be the mean and amplitude of each sinusoid fit, and m be the disattenuation multiplier determined above, then we can define $\tau_{max} = \tau_{mean} + m\tau_{amp}$ and $\tau_{min} = \tau_{mean} - m\tau_{amp}$.

Then if $\delta_{\mathbf{R}}$ and $\delta_{\mathbf{v}}$ are respectively the declinations of **R** and **v**, then $\delta_{\mathbf{v}}$ can be found by solving,

$$\frac{\tau_{min}}{\tau_{max}} = -\frac{cos(\delta_{\mathbf{v}} + \delta_{\mathbf{R}})}{cos(\delta_{\mathbf{v}} - \delta_{\mathbf{R}})} \tag{4}$$

And wave speed relative to Earth is then,

$$s = \frac{|\mathbf{R}|\, cos(\delta_{\mathbf{v}} - \delta_{\mathbf{R}})}{\tau_{max}} \tag{5}$$

We accordingly found declinations and speeds for the eight points shown in Fig. 5.

9 Fitting a 3-space orbital aberration ellipse

Of the eight points shown in Fig. 5, the five which lie within ±2.0 RA hours of the 3-space orbital aberration curve were found to represent waves with incoming directions and speeds as shown by Table 2. These directions are plotted as the large points in Fig. 6 and form a circular pattern that looks related to Earth orbit effects.

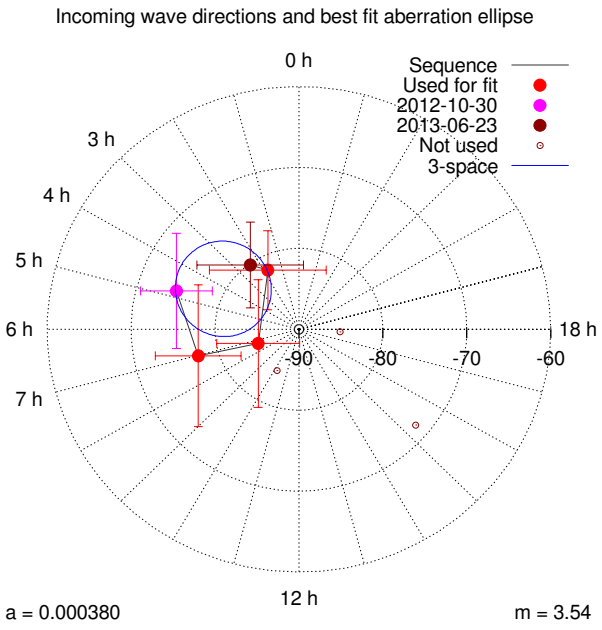

Fig. 6: Each point shows the incoming RA and declination of 3-space waves on a particular day. The blue ellipse shows a 3-space orbital aberration ellipse that has been fit to five points to minimize a chi-square for RAs and declinations. The closeness of the fit suggests that wave velocities on these days were approximately parallel to the direction of 3-space flow.

Then in view of the concordance between wave and 3-space RAs it might be possible to use the incoming wave directions as proxies for incoming 3-space flow directions.

To test this, Expression (3) was used to fit a 3-space orbital aberration ellipse to the wave directions so as to minimize a chi-square for RAs and declinations. The best fit shown in Fig. 6 was obtained using the incoming galactic flow velocity shown in the upper row of Table 3.

Table 2: Incoming Wave Directions and Speeds

Date	RA (hrs)	dec (deg)	speed (km/s)
2012-10-30	4.8 ± 1.8	−74.7 ± 3.8	505 ± 15
2013-01-27	7.0 ± 2.8	−77.6 ± 4.7	535 ± 18
2013-02-25	7.3 ± 6.1	−84.8 ± 4.3	574 ± 16
2013-05-24	1.8 ± 3.5	−81.8 ± 3.9	525 ± 14
2013-06-23	2.4 ± 2.9	−80.2 ± 3.8	507 ± 13

Table 3: Estimates of Incoming Galactic Flow Velocity

Ref.	RA (hrs)	dec (deg)	speed (km/s)
This paper	4.00 ± 0.51	−79.8 ± 1.0	500 ± 113
[2]	4.29	−75	486

For comparison the lower row shows the galactic flow velocity obtained from [2]. The closeness of the determinations suggests the wave directions may have served as reasonable proxies for direction of 3-space flow.

10 Probability calculation

Comparing Table 2 with Fig. 6 shows that the declinations have placed the five large points in correct sequence for an orbital aberration ellipse. Stating with any point, the probability of the other four being in correct sequence is $(\frac{1}{2})^4 = 1/16$.

Combining this with the 0.0046 probability for the distribution of RAs shown in Fig. 5, gives a combined probability for the five of the eight points shown in Fig. 6 to be arranged as they are of $p = 0.0046 \times \frac{1}{16} < 0.0003$.

11 Conclusions

We have been able to extract long range REG-REG correlations consistent with those reported in [1] and have also been able to estimate the velocities of 3-space waves and 3-space flow and observe earth orbit aberration effects. Our estimate of galactic 3-space flow velocity derived from REG-REG correlations is consistent with the value determined in [2] by combining optical fiber light-speed data with spacecraft Earth-flyby radar doppler-shift data.

Acknowledgements

Special thanks are owed to GCP [4] and its director Dr. Roger Nelson for enabling access to valuable data from the GCP network of REG devices.

References

[1] Cahill R.T. Nanotechnology Quantum Detectors for Gravitational Waves: Adelaide to London Correlations Observed. *Progress in Physics*, 2013, v. 4, 57-62.

[2] Cahill R.T. Combining NASA/JPL one-way optical-fiber light-speed data with spacecraft Earth-flyby Doppler-shift data to characterise 3-space flow. *Progress in Physics*, 2009, issue 4, 50-64.

[3] Cahill R.T. The dynamical velocity superposition effect in the quantum-foam theory of gravity. In: *Relativity, Gravitation, Cosmology: New Developments*, Dvoeglazov V., ed., Nova Science Pub., New York, 2009.

[4] The Global Consciousness Project http://global-mind.org/

[5] Bannister R.N. A guide to computing orbital positions of major solar system bodies: forward and inverse calculations http://www.met.rdg.ac.uk/~ross/Documents/OrbitNotes.pdf http://www.met.rdg.ac.uk/~ross/Astronomy/Planets.html